N-hydroxyphthalimide-TiO$_2$ complex visible light photocatalysis

Huimin Hao[a], Ji-Long Shi[a], Hui Xu[a], Xia Li[a], Xianjun Lang[a,b,*]

[a] College of Chemistry and Molecular Sciences, Wuhan University, Wuhan 430072, China
[b] Key Laboratory of Advanced Energy Materials Chemistry (Ministry of Education), Nankai University, Tianjin 300071, China

ARTICLE INFO

ABSTRACT

TiO$_2$ is the most established semiconductor photocatalyst. The prominence of TiO$_2$ is becoming increasingly obvious because its interfacial redox reactions have implication on a wide range processes such as energy conversion and environmental remediation. Herein, we exploited the surface complex created by the interaction between organic molecules with binding sites and accommodating surface of TiO$_2$ for visible light-driven selective aerobic oxidation reactions. A novel surface complex formed between N-hydroxyphthalimide (NHPI) and TiO$_2$ was discovered. The NHPI-TiO$_2$ complex turned out to be an outstanding visible light photocatalyst and was successfully used in the selective oxidation of amines into imines with atmosphere O$_2$ under blue LED irradiation. The stability of the NHPI-TiO$_2$ complex was preserved by 3 mol% of (2,2,6,6-tetramethylpiperidin-1-yl)oxyl (TEMPO) acting as a cooperative catalyst. Moreover, selectivities for the imine products were also promoted by TEMPO. Superoxide anion radical (O$_2$·$^-$) were evidenced to be the primary reactive oxygen species (ROS) to execute the oxidative conversions. This work suggests that TiO$_2$ surface complexes can be robust photocatalysts for visible light-driven selective aerobic reactions, provided that an appropriate cooperative redox catalyst exists to channel the photocatalytic electron transfer.

1. Introduction

TiO$_2$ has been one of the most widely used metal oxide materials in applications such as plastics, cosmetics, printing inks, food and a pigment for paints. This is mainly due to its physical properties of white colour, economic viability and chemical inertness. The seminal discovery that TiO$_2$ could implement the ultraviolet (UV)-assisted splitting of water into H$_2$ and O$_2$ ushered a new era of development for harnessing solar energy into clean chemical energy based on this material [1]. Gradually, the surface of TiO$_2$ can be transformed into an efficient platform for redox chemical reactions under the illumination of UV light [2]. Thereafter, under intensive research effort, many different types of semiconductor photocatalysts are discovered. However, interest in TiO$_2$ materials has never declined because TiO$_2$ possesses excellent activity, stability and non-toxicity that were unmatched by most of other photocatalysts. Thus it is still the focus of attention as a photocatalyst that can meet the grand challenges of energy and environment.

In semiconductor photocatalysis, the absorption of photons with energy larger than the bandgap of the semiconductor creates excitons (electron and hole pairs) which ultimately separate into electrons and holes that carry out reduction and oxidation reactions. However,

because of its wide bandgap, TiO$_2$ can only absorb UV light. Thus visible light, the most abundant component of sunlight, cannot be fully utilized, resulting in the limited applications of TiO$_2$ photocatalyst in many circumstances. To surmount this explicit deficiency, many attempts have been made to extend the absorption range of TiO$_2$ derived materials to the visible light region by various strategies [3]. Many prior reports focused on the doping of TiO$_2$ with transition metals such as Fe [4], Co [5] and Pt [6], La [7] and La/Sn [8] to succeed in this target. Later on, non-metal doped TiO$_2$ was proven to be a more productive strategy [9,10]. For example, C-doped TiO$_2$ can aid in the photoelectrochemical splitting of water [11]; N-doped TiO$_2$ was applied in the photodegradation of organic dye [12]; S-doped core-shell nanostructured rutile TiO$_2$ was exploited for hydrogen production [13]. These photocatalytic activities were all achieved under visible light illumination. Among of them, N-doped TiO$_2$ has a sensitive response to visible light and stimulates considerable attention given the conclusion that nitrogen is a superior doping element [14]. However, the nature of N-doping in TiO$_2$ is still under intensive debate which in turn jeopardize its further improvement in photocatalytic activity at the visible light region. It was necessary to establish an insightful understanding of N-doped TiO$_2$. The visible light activity of N-doped TiO$_2$ was usually attributed to bandgap engineering which is the most prevalent

* Corresponding author at: College of Chemistry and Molecular Sciences, Wuhan University, Wuhan 430072, China.
  E-mail address: xianjunlang@whu.edu.cn (X. Lang).

explanation [15]. Recently, it was proposed that surface sensitization of TiO$_2$ by N-containing species underpins the visible light activity [16]. This might explain the underlying visible light activity for many reported N-TiO$_2$. Thus we wanted to seek out examples of practical application with this concept to verify its validity. Amongst different future direction of travel, TiO$_2$ photocatalytic organic transformations has become increasingly important which can advance an environmentally friendly alternative in synthetic methods. Oxidative reactions are pivotal in nature and fundamental transformations in chemical reactions. The development of selective, feasible, sustainable, and environmentally friendly oxidation reactions is one of biggest challenges nowadays. In order to meet these requirements, a wide variety of visible light photocatalysts have emerged and rapidly progressed, of which TiO$_2$ is the most promising candidate [17,18].

Previously, we applied this concept of N-species surface sensitization on TiO$_2$, with pure TiO$_2$ as the reaction platform, for visible light-driven selective oxidation of amines [19], synergistic selective oxidation of amines and sulfides [20], and tertiary amine promoted selective oxidation of sulfides [21]. The visible light activities were all caused by the Lewis base and acid interaction between amine and TiO$_2$. Still, the N-species of these amines cannot permanently stay at the surface of TiO$_2$. This scenario cannot be served as a direct model because it is quite different from N-TiO$_2$. Thus we envisioned that one should find N-containing molecules that can be connected with the surface hydroxyl groups of TiO$_2$ with covalent bonding. The immobilization of hydroxylamine on the surface of TiO$_2$ might be a better model for N-TiO$_2$. Nevertheless, hydroxylamine is a very potent reducing agent which is therefore not stable under photocatalytic oxidative conditions. Thus one should bury it with stable molecular motif to prevent it from destruction under aerobic oxidation conditions. Phthalic acid should be an attractive molecular motif for this purpose. Actually, phthalic acid can react with hydroxylamine to produce NHPI. For the convenience of a more unequivocal model, we commenced this study from NHPI to understand the surface sensitization of TiO$_2$.

NHPI is an eminent organocatalyst for selective aerobic oxidation of many types of organic compounds [22], suggesting it is relatively stable under the assaults of ROS. NHPI seems an attractive model molecule to investigate the doping nature of N-TiO$_2$. However, to the best of our knowledge, there is no previous report regarding the NHPI-TiO$_2$ complex, detailing their interaction and consequences. Moreover, NHPI is the *N*-hydroxy derivative of phthalimide, and can generate *N*-oxyl radical via one oxidation step of abstracting H from NHPI [23]. Adopting organics to modify the surface of semiconductors was prove to be a successful route for enhancing the activities of photocatalysts [24–26]. As part of our continuing effort in this area, we herein report that the discovery and characterization of the NHPI-TiO$_2$ complex which can absorb light at visible region. The visible light absorption is caused by the ligand-to-metal charge transfer [27,28] that can be considered as N-single site active centre, a situation quite similar to that of the single site catalyst [29].

Subsequently, we took advantage of this novel complex for the photocatalytic selective oxidation of amines into imines with atmosphere O$_2$. In terms of substrate, 0.5 mol% of NHPI and 3 mol% of TEMPO were needed to complete the selective aerobic oxidation of amines into imines. This is the first example of N−OH as the binding site to construct surface complex and NHPI was applied as the monodentate surface binding ligand of TiO$_2$ surface for selective aerobic oxidation reaction. Hopefully, surface complex visible light photocatalysis can be diversified into uncovering of more surface ligands and adding avantgarde redox reaction dimensions.

2. Experimental

2.1. Preparation of N-hydroxyphthalimide-TiO$_2$ complex (NHPI-TiO$_2$)

The procedure for the preparation of NHPI-TiO$_2$ was as follows: 3 g

anatase TiO$_2$ (Ishihara ST-01) was put into a 50 mL beaker containing 20 mL CH$_3$CN for 10 min of ultrasonication to disperse TiO$_2$ uniformly. Then, 0.09 mmol NHPI was put into the dispersed TiO$_2$ in CH$_3$CN for a further 10 min ultrasonication. After that, the mixture was magnetically stirred at 500 rpm for 12 h under dark conditions. Then, NHPI-TiO$_2$ was collected with a rotary evaporator equipped with a vacuum pump. The TEM, HRTEM, XPS, PXRD and UV–vis spectra characterizations and the instrumental conditions were presented in the supplementary data (Figs. S1–S4).

2.2. Typical procedure for the photocatalytic selective aerobic oxidation of amine

First, 50.3 mg NHPI-TiO$_2$, 0.009 mmol TEMPO, 0.3 mmol benzylamine and 1 mL CH$_3$CN were placed in a 10 mL Pyrex reactor for 5 min ultrasonication. Second, the mixture was stirred in the dark for 1 h to reach adsorption-desorption equilibrium. Third, put the Pyrex reactor in magnetic stirring apparatus. Mixture in the Pyrex reactor was stirred at 1500 rpm and irradiated with 3 W blue light-emitting diodes (LEDs) (Shenzhen Ouying Lighting Science and Technology Co., Ltd.). The butyl rubber septum for the Pyrex reactor was punched a hole by a rubber hole puncher to connect with air to supply oxidant for the system. The temperature of the reaction system was controlled at 25 °C. Finally, the photocatalyst nanoparticles were separated from the reaction mixture by centrifugation. And the reaction product was analyzed by gas chromatography equipped with a flame ionization detector (GC-FID) using chlorobenzene as the internal standard. The structures of products were confirmed by comparison with the retention time with authentic samples by GC-FID and further confirmed by gas chromatography–mass spectrometry (GC–MS). The instrumental conditions and analysis details were provided in the supplementary data.

3. Results and discussion

Recently, we have shown that catechol and its derivatives can be selected as the molecule to construct the surface complex with TiO$_2$ for the selective oxidation of amines into imines with air [30]. Trying to better this previous reported system, we expanded the surface complex photocatalyst system with a new molecule, NHPI. NHPI was involved in several photocatalytic systems as a co-catalyst [23] and has been proved, in its own right, as photocatalyst for oxidative transformations [31,32]. But the interaction between NHPI and TiO$_2$ which could be a model for N-TiO$_2$ received attention. The combination of NHPI and α-Fe$_2$O$_3$ can perform the photocatalytic oxygenation of sp^3 C−H with O$_2$ which is attributed to the long-lived *N*-oxyl radical, phthalimide N-oxyl radical (PINO*) from the fixation of α-Fe$_2$O$_3$ and stable nitrogen belongs to NHPI [33]. Since the confinement of NHPI onto metal oxide is strong, we envisioned that the hydroxyl group of NHPI combines with TiO$_2$ through strong chemical bonds successfully (Eq. 1.

$$(1)$$
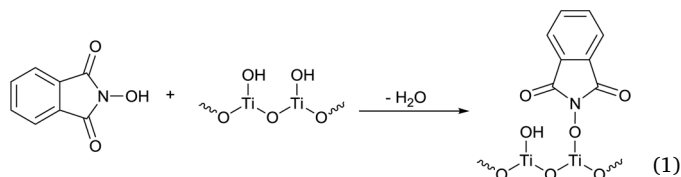
NHPI is a colorless, odorless crystalline powder and the color of TiO$_2$ nanoparticles is white. When we put NHPI into TiO$_2$ suspension in acetonitrile, a deepening of the yellow color could be observed by naked eyes, suggesting the formation of a surface complex. The transmission electron microscope (TEM) images of NHPI-TiO$_2$ and TiO$_2$ (Fig. S1) have been collected, indicating that the surface modification of TiO$_2$ with NHPI does not influence the structure of anatase TiO$_2$. And X-ray photoelectron spectra (XPS) of NHPI-TiO$_2$ (Fig. S2) show that the peaks exist similarly compared with the N-doped TiO$_2$, therefore serving a good model system in scale. We thus further characterized the
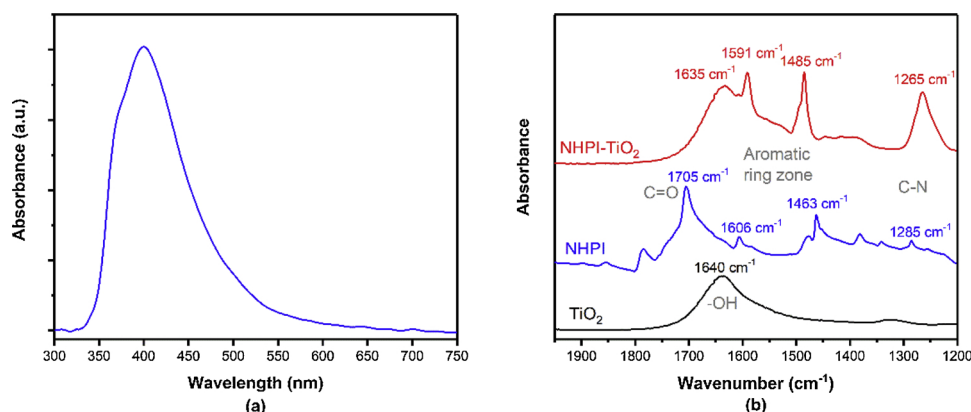
Fig. 1. (a) The UV–vis light absorbance spectrum of NHPI-TiO$_2$ complex; (b) the ATR-FTIR spectra of TiO$_2$, NHPI and NHPI-TiO$_2$ complex.

Table 1
The influence of different semiconductors on the visible light-driven selective oxidation of benzylamine by merging NHPI-TiO$_2$ complex photocatalysis with TEMPO catalysis[a].

Entry	Semiconductors	Suppliers	Conv. [%][b]	Sel. [%][b]
1	ST-01 Anatase	Ishihara	73	98
2	AEROXIDE P25	Evonik	51	98
3	Anatase	Alfa Aesar	54	98
4	ZnO	Aladdin	0	–

[a] Reaction conditions: benzylamine (0.3 mmol), Metal oxides (50 mg), NHPI (1.5 × 10^{-3} mmol), TEMPO (9 × 10^{-3} mmol), air (1 atm), blue LED irradiation (3 W × 4), CH$_3$CN (1 mL), 30 min.
[b] Determined by GC-FID using chlorobenzene as the internal standard, conversion of benzylamine and selectivity of *N*-benzylidenebenzylamine.

NHPI-TiO$_2$ complex with UV–vis and attenuated total reflectance Fourier transform infrared spectra (ATR-FTIR) (Fig. 1). Fig. 1 a shows the UV–vis absorbance of the NHPI-TiO$_2$ complex after subtracting the absorbance of TiO$_2$ with a peak at 400 nm and an extension upto 550 nm in the visible region, giving evidence to the formation of visible light absorbing complex. To further confirm the state of attached NHPI on TiO$_2$ surface, ATR-FTIR measurement was carried out (Fig. 1b). The peak at 1705 cm^{-1} which belongs to the carbonyl (−C=O) vibration of NHPI is invisible in the NHPI-TiO$_2$ complex because it becomes coincident with the hydroxyl (−OH). That is to say, it occurs bathochromic shift rather than disappearing in the NHPI-TiO$_2$ complex. Reasonably, there is an interaction between the −C=O of NHPI and the surface of TiO$_2$ in the complex. The shift of aromatic ring skeleton vibration (from 1606 to 1591 cm^{-1}; from 1463 to 1485 cm^{-1}) suggests that aromatic ring of NHPI has adsorbed on the surface of TiO$_2$. The peak at 1285 cm^{-1} moves to 1265 cm^{-1}, and it demonstrates the influence on C−N bond from the formation of NHPI-TiO$_2$ complex. Based on previous FTIR studies of NHPI fixed on α-Fe$_2$O$_3$ [33] and molecular titanium-hydroxamate complexes [34], we could deduce that NHPI can be anchored on TiO$_2$ and the aromatic molecular motif lies down on the surface of TiO$_2$ and connects to the surface hydroxyl group via covalent bonding.

We designed the new surface complex NHPI-TiO$_2$, trying to employ it for the oxidative conversion of organic molecules under visible light irradiation. With regard to the present new surface complex of NHPI-TiO$_2$, the BET specific surface area is 255 m^2 g^{-1}. And powder X-ray diffraction (PXRD) characterization was demonstrated in Fig. S3, indicating the modification does not influence the anatase phase of TiO$_2$. Based on the results of diffuse reflection UV–vis spectroscopy (Fig. S4), we detailed seven different LEDs for the visible light-driven selective oxidation of benzylamine (Table S1) and ultimately determined that blue LEDs have the best photocatalytic effect in the present system.

Next, we uncovered CH$_3$CN is the most excellent one in the tested solvents (Table S2), delivering the highest conversion of benzylamine and high selectivity of *N*-benzylidenebenzylamine.

TiO$_2$ is one of the important members in this surface complex. The photocatalytic performance of the surface complexes from different kinds of TiO$_2$ has been displayed in Table 1 (entries 1–3). On the one hand, three types of complexes all could promote the selective oxidation of benzylamine as photocatalysts. We have reasons to believe that the formations of these surface complexes between NHPI and TiO$_2$ are of generality. On the other hand, in view of their different photocatalytic activities, ST-01 TiO$_2$ was proved to be the optimal one and screened out for the later experiments. Besides, we carried out experiments with other semiconductor, such as ZnO. Conversion of benzylamine did not occur (entry 4, Table 1).

Any component of the present experimental system is essential, which is well proven in the results of the control experiments (Fig. 2). The benzylamine cannot be converted without any other member in the present photocatalytic scheme (Fig. 2a). Among TiO$_2$, NHPI or TEMPO, none of them can work independently (Fig. 2b–d). This visible light photocatalytic reaction system is inactive and the reaction cannot proceed at all in the absence of TiO$_2$ (Fig. 2e). When NHPI or TEMPO was not added into the experimental system, the conversion was seriously inhibited compared with standard condition (Fig. 2f–g). Thence, there is a conclusion that any one plays a significant role in conducting the experiment. The conversion of substrate in this reaction system is close to zero in the case of lacking light irradiation (Fig. 2, i). It is evident that visible light is the indispensable driving force for this reaction.

As a benign oxidant, molecular oxygen (O$_2$) has been gaining in popularity. In our opinion, the influence of the initial O$_2$ pressure on the oxidation of benzylamine is worth considering. When the initial O$_2$ pressure increases from 0.2 atm to 2.5 atm, the visible light-driven
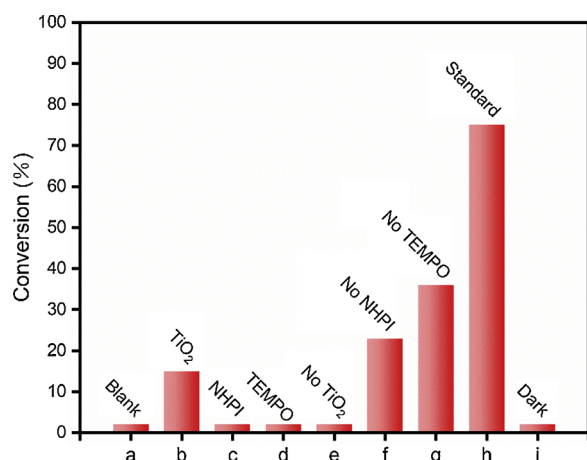
Fig. 2. Control experiments for the selective oxidation of amines to imines. (a) blank reaction; (b) TiO_2 only; (c) NHPI only; (d) TEMPO only; (e) without TiO_2; (f) without NHPI; (g) without TEMPO; (h) standard conditions; (i) dark condition.
Standard conditions: benzylamine (0.3 mmol), TiO_2 (50 mg), NHPI (1.5×10^{-3} mmol), TEMPO (9×10^{-3} mmol), air (1 atm), CH_3CN (1 mL), blue LED irradiation ($3 W \times 4$), 30 min. Conversions of benzylamine were determined by GC-FID using chlorobenzene as the internal standard.
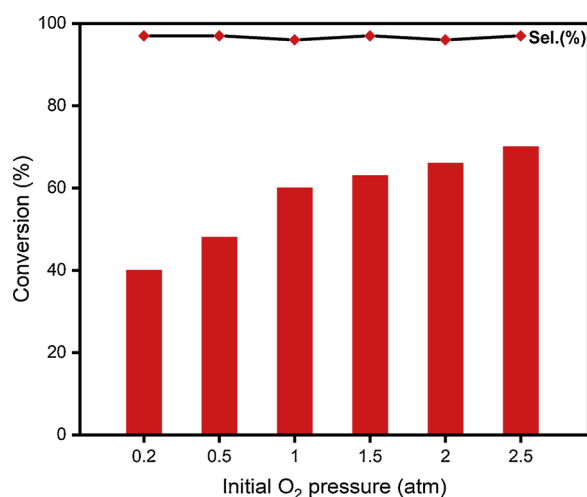
Fig. 3. The influence of the initial O_2 pressure on the visible light-driven selective oxidation of benzylamine by merging NHPI-TiO_2 complex photocatalysis with TEMPO catalysis.
Reaction conditions: benzylamine (0.3 mmol), TiO_2 (50 mg), NHPI (1.5×10^{-3} mmol), TEMPO (9×10^{-3} mmol), blue LED irradiation ($3 W \times 4$), CH_3CN (1 mL), 20 min. Conversion of benzylamine, and selectivity of *N*-benzylidene-benzylamine were determined by GC-FID using chlorobenzene as the internal standard.

selective oxidation of benzylamine became faster apparently up to 1 atm but showed an almostly flat trend from 1.5 atm to 2.5 atm (Fig. 3). This phenomena is different from thermal reaction in which high pressure of O_2 always delivers better results for activation of O_2. Since the present photocatalytic reaction was carried out at room temperature, the interaction of TiO_2 to O_2 saturated at a certain pressure of O_2.

Table 2
Quenching experiments to determine the ROS for the visible light-driven selective oxidation of benzylamine by merging NHPI-TiO_2 complex photocatalysis with TEMPO catalysis[a].

Entry	Quencher (equiv.)	Roles	Conv. [%][b]
1	N_2 (–)	O_2 replacement	4
2[c]	*p*-BQ (0.2)	$O_2^{\cdot-}$ scavenger	6
3	$AgNO_3$ (1)	electron scavenger	6
4[d]	CD_3CN (–)	singlet oxygen maintainer	75

[a] Reaction conditions: benzylamine (0.3 mmol), TiO_2 (50 mg), NHPI (1.5×10^{-3} mmol), TEMPO (9×10^{-3} mmol), air (1 atm), blue LED irradiation ($3 W \times 4$), CH_3CN (1 mL), 30 min.
[b] Determined by GC-FID using chlorobenzene as the internal standard, conversion of benzylamine.
[c] *p*-BQ, *p*-benzoquinone.
[d] CD_3CN (1 mL).

In order to determine the ROS for the photocatalytic oxidation, we carried out several quenching experiments. When the system lacks O_2, it is equal to the lack of oxidants. So the reaction cannot occur (entry 1, Table 2). It is no doubt that O_2 provides the possibility for the selective aerobic oxidation of benzylamines. Adding *p*-BQ as the $O_2^{\cdot-}$ scavenger and $AgNO_3$ as the e_{cb}^- trapping agent, both actions prevent the reaction entirely (entries 2–3, Table 2), which implies that the primary ROS for the visible light-driven photocatalytic oxidation of benzylamines is $O_2^{\cdot-}$. The conversion rate of the reaction did not increase significantly when using CD_3CN as the solvent (entry 4, Table 2). Together with the previous result (entry 2, Table 2), one can indirectly reckon that the ROS for the selective aerobic oxidation of benzylamines is $O_2^{\cdot-}$ rather than singlet oxygen.

For the purpose of exploring the mechanism of the reaction, we conducted *in-situ* electron spin resonance (ESR) test (Fig. 4). The 5,5-Dimethyl-1-Pyrroline *N*-oxide (DMPO) was adopted as the trapper of $O_2^{\cdot-}$ and ESR signals denote the accumulation of trapped $O_2^{\cdot-}$. An obviously increasing signal with time (Fig. 4a) suggests that visible light induces a continuous stream of reactive oxygen species $O_2^{\cdot-}$, which is an intuitive and powerful proof of the previous conclusions about the ROS for the reaction. Fig. 4b reveals that the amount of TEMPO will reduce in pace with the reaction proceeding due to a part of TEMPO transformed into ESR sluggish species. The signal of TEMPO shows a certain recovery when the light is turned off (Fig. 4b), wherefore it is rational that we speculate there is a circulation among TEMPO, TEMPOH and TEMPO$^+$.
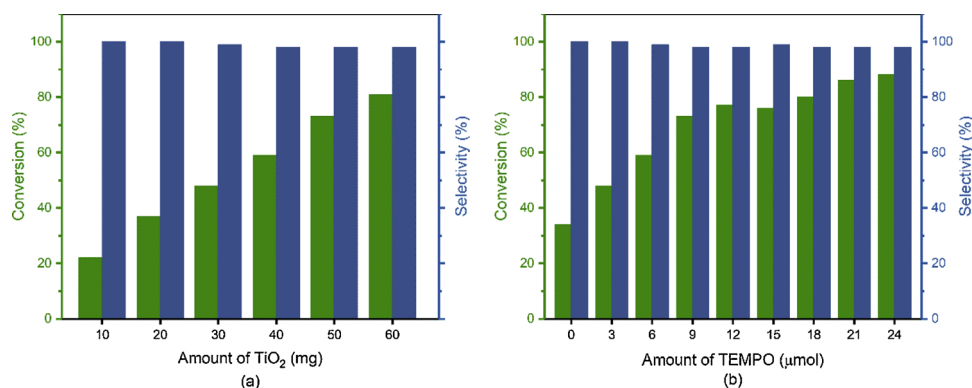
The influence of the amount of TiO_2 on the oxidation of benzylamine can be proved in Fig. 5. The conversion of the reaction increases regularly with the uniform increase of the amount of TiO_2 (Fig. 5a), which firmly verifies that TiO_2 together with NHPI forms the surface complex rather than a simple supportive role. Conversely, with the multiple increase of TEMPO, the conversion of benzylamine shows a sharp rise at the beginning but a gradual steady trend subsequently (Fig. 5b). In comparison to TiO_2, TEMPO acts as co-catalyst and just converts among TEMPO, 2,2,6,6-tetramethylpiperidin-1-ol (TEMPOH) and 2,2,6,6-tetramethylpiperidine-1-oxoammonium (TEMPO$^+$) instead of being consumed. To verify our speculation, we adopted same amount of TEMPOH in place of TEMPO, and the reaction achieved better conversion and equivalent selectivity (Eq. 2). This result is also in good agreement with that of ESR spectra (Fig. 4b).
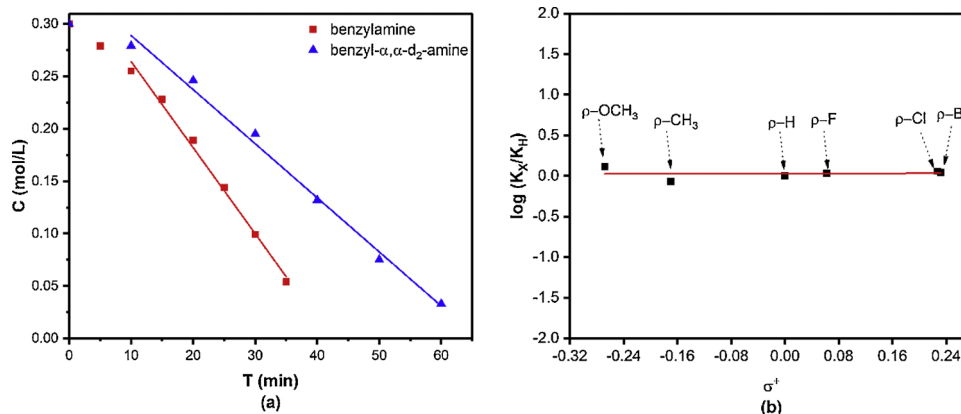

3 mol% TEMPO, Conv. 73%, Sel. 98%
3 mol% TEMPOH, Conv. 83%, Sel. 97%
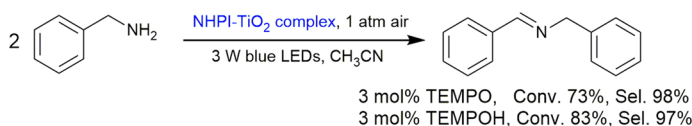
(2)
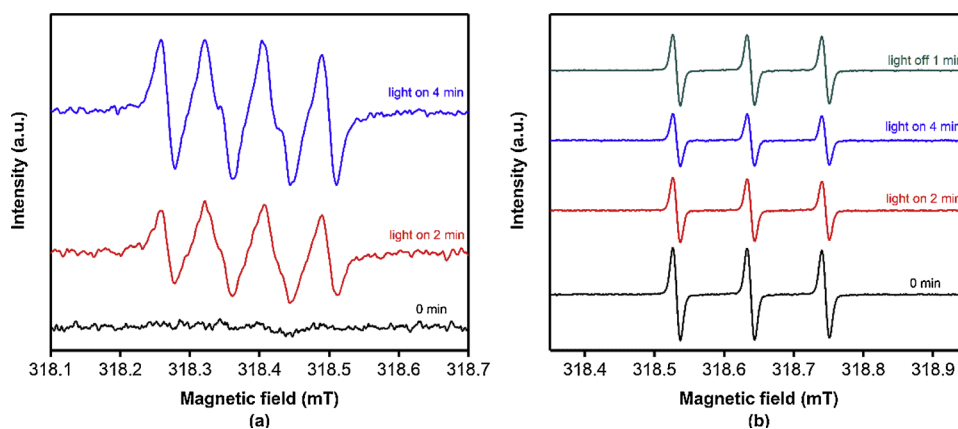
Fig. 4. The ESR spectra recorded during the selective oxidation of benzylamine by NHPI-TiO$_2$ complex photocatalysis (a) spin trapping of superoxide anion radical (O$_2$·$^-$) with DMPO, (b) TEMPO.

Fig. 5. (a) The influence of the amount of TiO$_2$; (b) The influence of the amount of TEMPO on the visible light-driven selective aerobic oxidation benzylamine to imine with air by merging NHPI-TiO$_2$ complex photocatalysis with TEMPO catalysis.

Reaction kinetic studies for the photocatalytic selective aerobic oxidation of benzylamine were executed. We believed that the formation process of the photocatalyst needs to undergo an induction period due to the presence of points in the front of the kinetic curve. Thus, the curves started at 10 min in Fig. 6. It turns out that this visible light photocatalytic selective oxidation of benzylamine follows zero-order

reaction (Fig. 6a), of which reaction rate constant k_H is 0.00821 mol L^{-1} min^{-1}. This phenomenon is similar for the selective oxidation of both benzylamine and benzyl-α,α-d$_2$-amine. Then the reaction rate constant k_D of the selective oxidation of benzyl-α,α-d$_2$-amine is acquired as 0.00516 mol L^{-1} min^{-1}. The kinetic isotope effect value is 1.59 and it does not show evident first-order isotope effect. From

Fig. 6. (a) Reaction kinetic plots of the selective oxidation of benzylamine and benzyl-α,α-d$_2$-amine by merging the visible light photocatalysis of NHPI-TiO$_2$ complex with TEMPO using air as the oxidant; (b) Hammett plot for the photocatalytic selective aerobic oxidation of *para*-substituted benzylamines.
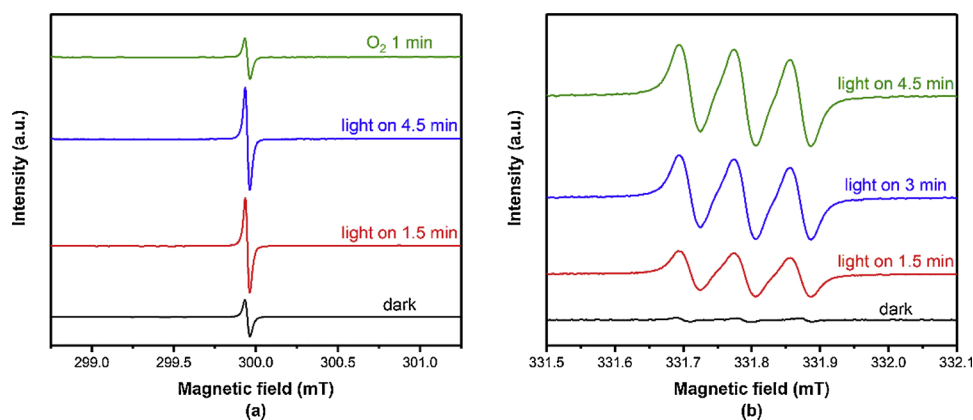
Fig. 7. The ESR spectra recorded during NHPI-TiO$_2$ complex photocatalysis (a) conduction band electrons; (b) PINO.
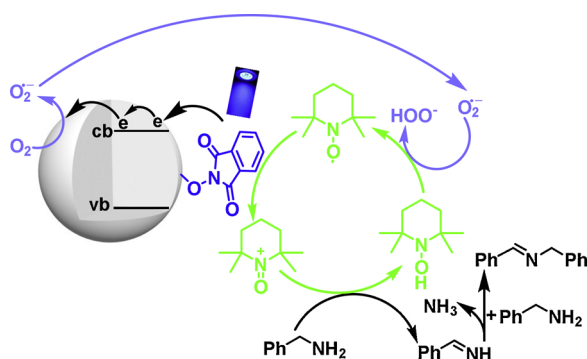
Fig. 8. The plausible mechanism for the visible light-driven selective oxidation of benzylamine with air by merging NHPI-TiO$_2$ complex photocatalysis with TEMPO catalysis.

Fig. 6b, Hammett plot for the oxidation of *para*-substituted benzylamines depicts a nearly horizontal line and reveals that a neutral free radical partook in the reaction progresses further, validating proton coupled electron transfer rather than hydride abstraction is the key step in the oxidation of benzylamine.

To acquaint the procedures of reaction better, the conduction band electrons (e_{cb}^-) and PINO* have been detected through ESR measures (Fig. 7). In the absence of O$_2$ and visible light, the normal state of e_{cb}^- was obtained. With the prolonging of illumination time, the signal of conduction band electron exhibits an increasing tendency. It reveals that extra conduction band electrons were excited and accumulated under visible light irradiation. When the O$_2$ participates in the system, the signal of e_{cb}^- becomes much weaker which was attributed to the transfer of electrons from conduction band of TiO$_2$ to O$_2$. Simultaneously, the PINO* was captured by ESR technique as well (Fig. 7b). It was confirmed that the photocatalytic reaction process involved the production of PINO*.

Taking all the aforementioned experimental results into account, we rationalized a plausible mechanism for the visible light-driven selective aerobic oxidation of benzylamine by merging NHPI-TiO$_2$ complex photocatalysis with TEMPO catalysis in Fig. 8. The adsorption of NHPI onto the surface of anatase TiO$_2$ gives rise to the formation of NHPI-TiO$_2$ complex. The absorption of this complex overlaps the lighting emitting spectrum of the blue LED. Under blue LED irradiation, electron transfers from the NHPI motif to the conduction band of TiO$_2$, creating e_{cb}^- and *N*-oxyl radical PINO* which further drives the adaptation of
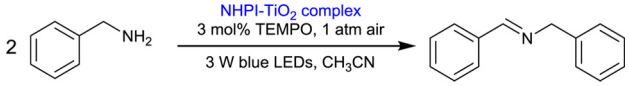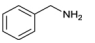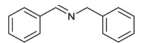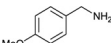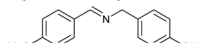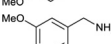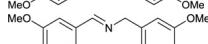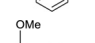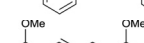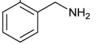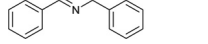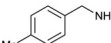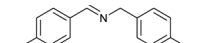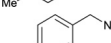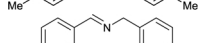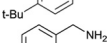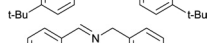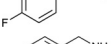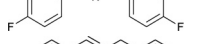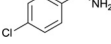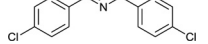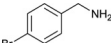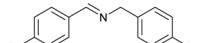
TEMPO to TEMPO$^+$. TEMPO$^+$ instigates two-electron oxidation of benzylamine into phenylmethanimine, affording TEMPOH. Meanwhile e_{cb}^- initiates one-electron reduction of O$_2$ to O$_2^{\cdot-}$. Phenylmethanimine condensates with benzylamine into the final imine product; O$_2^{\cdot-}$ accepts a second electron and a proton from TEMPOH to restore TEMPO, affording the final H$_2$O$_2$ by combining with a second proton from the substrate.

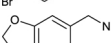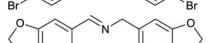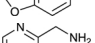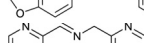At last, we explored the catholicity of this protocol. A plethora of substituted primary amines was chosen for their selective aerobic oxidation and a gratifying outcome was obtained (Table 3). When CH$_3$O-group substitutes in the *meta* position, slight higher conversion is discovered comparing to the *para* and *ortho* position (entries 2–4, Table 3). Afterwards, we picked several *para*-substituted amines with different electronic effects to check the reactivities (entries 5–9, Table 3). It can be concluded that there is no significant difference between the amines including electron-withdrawing groups and the electron-donating groups. Therefore, the electron effect of substituent group about this protocol seems to be relatively weak. In addition, heteroatom-containing amines can also get satisfactory conversion (entries 10–12, Table 3). Afterwards, we performed the recycle reactions, and conversions decreased from 73% to 70% after three cycles, affirming that the complex photocatalyst has good stability. When the amount of the substrate expands four-fold to 1.2 mmol, excellent conversion and selectivity can be gained (entry 13, Table 3) and the isolated yield is 93% (see supplementary information S6). In short, the present photocatalytic system is quite efficacious and extendable.

4. Conclusions

To sum up, we have designed a novel surface complex of NHPI-TiO$_2$ as the photocatalyst with excellent activity and successfully employed it to the selective oxidation of amines into imines with high conversions and high selectivities. It is worth mentioning that the design and synthesis of this surface complex is instructive to our understanding of the visible light photocatalyst of N-doped TiO$_2$. Notably, applying NHPI-TiO$_2$ complex with TEMPO as a co-catalyst for the photocatalytic selective aerobic oxidation of amines is a beneficial and creative protocol for the follow-up understanding surface complex photocatalysis. Surface complex photocatalysis, along with our previous strategy of organic dye-sensitized TiO$_2$ photocatalysis [35–37], underpins the surface modification of TiO$_2$ can be a way forward for constructing photocatalytic selective aerobic oxidation reactions on the condition that a suitable cooperative catalyst has existed.

Table 3
Visible light-driven selective oxidation of amines to imines with air by merging NHPI-TiO$_2$ complex photocatalysis with TEMPO catalysis[a].

Entry	Substrate	Product	T [min]	Conv. [%][b]	Sel. [%][b]
1			40	97	94
2			30	94	95
3			30	97	91
4			45	95	92
5			45	96	95
6			65	94	96
7			30	91	96
8			40	98	93
9			40	98	93
10			30	95	88
11			70	94	92
12			60	92	96
13[c]			130	99	93

[a] Reaction conditions: amine (0.3 mmol), TiO$_2$ (50 mg), NHPI (1.5×10^{-3} mmol), TEMPO (9×10^{-3} mmol), air (1 atm), blue LED irradiation (3 W × 4), CH$_3$CN (1 mL).
[b] Determined by GC-FID using chlorobenzene as the internal standard, conversion of benzylamine, selectivity of corresponding imine.
[c] benzylamine (1.2 mmol), TEMPO (3.6×10^{-2} mmol).

Acknowledgements

Appendix A. Supplementary data

Supplementary material related to this article can be found, in the online version, at doi:https://doi.org/10.1016/j.apcatb.2019.01.037.

References

[1] A. Fujishima, K. Honda, Nature 238 (1972) 37–38.
[2] X.J. Lang, W.H. Ma, C.C. Chen, H.W. Ji, J.C. Zhao, Acc. Chem. Res. 47 (2014) 355–363.
[3] V. Etacheri, C. Di Valentin, J. Schneider, D. Bahnemann, S.C. Pillai, J. Photochem. Photobiol. C: Photochem. Rev. 25 (2015) 1–29.
[4] L.F. Cui, Y.S. Wang, M.T. Niu, G.X. Chen, Y. Cheng, J. Solid State Chem. 182 (2009) 2785–2790.
[5] O. Ola, M.M. Maroto-Valer, Appl. Catal. A: Gen. 502 (2015) 114–121.
[6] S. Kim, S.J. Hwang, W. Choi, J. Phys. Chem. B 109 (2005) 24260–24267.
[7] Z.L. Shi, H. Lai, S.H. Yao, S.F. Wang, Chin. J. Chem. Phys. 25 (2012) 96–102.
[8] X.D. Zhu, L.X. Pei, R.R. Zhu, Y. Jiao, R.Y. Tang, W. Feng, Sci. Rep. 8 (2018).
[9] M.A. Mohamed, W.N.W. Salleh, J. Jaafar, A.F. Ismail, M. Abd Mutalib, S.M. Jamil, Carbohydr. Polym. 133 (2015) 429–437.
[10] M. Farbod, M. Kajbafvala, Appl. Catal. B: Environ. 219 (2017) 344–352.
[11] S.U.M. Khan, M. Al-Shahry, W.B. Ingler, Science 297 (2002) 2243–2245.
[12] R. Asahi, T. Morikawa, T. Ohwaki, K. Aoki, Y. Taga, Science 293 (2001) 269–271.
[13] C.Y. Yang, Z. Wang, T.Q. Lin, H. Yin, X.J. Lu, D.Y. Wan, T. Xu, C. Zheng, J.H. Lin, F.Q. Huang, X.M. Xie, M.H. Jiang, J. Am. Chem. Soc. 135 (2013) 17831–17838.
[14] H.J. Jung, S.H. Kye, H.J. Kang, H.J. Yang, J.B. Yoo, K.H. Lee, N.H. Hur, Appl. Catal. A: Gen. 558 (2018) 9–17.
[15] R. Asahi, T. Morikawa, H. Irie, T. Ohwaki, Chem. Rev. 114 (2014) 9824–9852.
[16] D. Mitoraj, H. Kisch, Angew. Chem. Int. Ed. 47 (2008) 9975–9978.
[17] M. Bellardita, F. Parrino, E.I. García-López, G. Marcì, V. Loddo, L. Palmisano, ACS Catal. 8 (2018) 11191–11225.
[18] F. Parrino, C. De Pasquale, L. Palmisano, ChemSusChem (2019), https://doi.org/10.1002/cssc.201801898.
[19] X.J. Lang, W.H. Ma, Y.B. Zhao, C.C. Chen, H.W. Ji, J.C. Zhao, Chem. Eur. J. 18 (2012) 2624–2631.
[20] X.J. Lang, W.R. Leow, J.C. Zhao, X.D. Chen, Chem. Sci. 6 (2015) 1075–1082.
[21] X.J. Lang, W. Hao, W.R. Leow, S.Z. Li, J.C. Zhao, X.D. Chen, Chem. Sci. 6 (2015) 5000–5005.
[22] F. Recupero, C. Punta, Chem. Rev. 107 (2007) 3800–3842.
[23] X.J. Lang, J.C. Zhao, Chem. Asian J. 13 (2018) 599–613.
[24] B.Y. Xu, Y. An, Y.Y. Liu, B.B. Huang, X.Y. Qin, X.Y. Zhang, Y. Dai, M.H. Whangbo, Chem. Commun. 52 (2016) 13507–13510.
[25] Z.Y. Jiang, Y.Y. Liu, T. Jing, B.B. Huang, Z.Y. Wang, X.Y. Zhang, X.Y. Qin, Y. Dai, Appl. Catal. B: Environ. 200 (2017) 230–236.
[26] B.Y. Xu, Y. An, Y.Y. Liu, X.Y. Qin, X.Y. Zhang, Y. Dai, Z.Y. Wang, P. Wang, M.H. Whangbo, B.B. Huang, J. Mater. Chem. A. 5 (2017) 14406–14414.
[27] G. Zhang, G. Kim, W. Choi, Energy Environ. Sci. 7 (2014) 954–966.
[28] W. Macyk, K. Szaciłowski, G. Stochel, M. Buchalska, J. Kuncewicz, P. Łabuz, Coord. Chem. Rev. 254 (2010) 2687–2701.
[29] A.Q. Wang, J. Li, T. Zhang, Nat. Rev. Chem. 2 (2018) 65–81.
[30] J.L. Shi, H.M. Hao, X. Li, X.J. Lang, Catal. Sci. Technol. 8 (2018) 3910–3917.
[31] A.K. Yadav, L.D.S. Yadav, Chem. Commun. 52 (2016) 10621–10624.
[32] M. Singh, A.K. Yadav, L.D.S. Yadav, R.K.P. Singh, Tetrahedron Lett. 59 (2018) 450–453.
[33] C.F. Zhang, Z.P. Huang, J.M. Lu, N.C. Luo, F. Wang, J. Am. Chem. Soc. 140 (2018) 2032–2035.
[34] B.J. Brennan, J. Chen, B. Rudshteyn, S. Chaudhuri, B.Q. Mercado, V.S. Batista, R.H. Crabtree, G.W. Brudvig, Chem. Commun. 52 (2016) 2972–2975.
[35] Y.C. Zhang, Z. Wang, X.J. Lang, Catal. Sci. Technol. 7 (2017) 4955–4963.
[36] Z. Wang, X.J. Lang, Appl. Catal. B: Environ. 224 (2018) 404–409.
[37] H.M. Hao, Z. Wang, J.L. Shi, X. Li, X.J. Lang, ChemCatChem 10 (2018) 4545–4554.